Deep-Sea Research, Vol. 29, No. 12A, pp. 1415 to 1436, 1982.
Printed in Great Britain.

0198–0149/82/121415–22 $03.00/0
© 1982 Pergamon Press Ltd.

Up–down resolution in ocean acoustic tomography

WALTER MUNK*† and CARL WUNSCH*‡

(*Received* 1 *February* 1982; *accepted* 17 *May* 1982; *final revision received* 2 *June* 1982)

Abstract—In a recent experiment (THE OCEAN TOMOGRAPHY GROUP, *Nature*, **299**, 121–125, 1982) the sound-speed field (and hence temperature) *within* an ocean volume was computed from acoustic travel times *through* the volume along many diverse ray paths, using inverse theory. Here we consider the limits on vertical resolution imposed by the fundamental character of the ocean sound channel. For a standard case we take an axial transmitter and receiver separated by 1000 km, with layers determined by the turning depths of double-looped rays. This gives an underdetermined system of 10 layers and six rays, with a forbidding up–down ambiguity between 'conjugate' layers (two layers with equal sound speed above and beneath the sound axis). The ambiguity can be reduced (but not eliminated) by including rays with an extra upper (or lower) loop, and can be removed by going to a coarse vertical grid. The results apply to the 'agnostic' case where nothing is prescribed: if it can be assumed that the disturbances are $N(z)$ weighted according to WKBJ theory, then the standard 10-layer case is adequately resolved in the upper and axial ocean. If one can prescribe that the disturbance is associated with only the gravest few modes (as found during the MODE expedition), then the results are favourable at all depths.

We consider tomography with reciprocal transmissions for obtaining the fields of both particle velocity and sound speed, and we assume that the density perturbations are adequately determined by the sound field using an average T–S relation. The thermal-wind equation relates the vertical velocity gradient to the horizontal density gradient and can be used to impose a constraint on the inversion process, which significantly improves the determination of both fields. The procedure leads to a formalism for objectively separating barotropic and baroclinic velocity fields.

INTRODUCTION

THERE are several methods (e.g., satellite altimetry) for obtaining good areal resolution at the ocean surface, but the problem of the downward extension of ocean-surface features into the deep interior is uniquely suited to acoustic probing, given the circumstances that the oceans are transparent to sound and opaque to electromagnetic waves.

In a previous paper (MUNK and WUNSCH, 1979; to be referred to as MW), we considered the measurement of the three-dimensional field of sound speed $C(x, y, z)$ *within* a volume by measuring the travel times of sound waves along many different paths *through* the volume. The full three-dimensional problem was separated into consideration of the field $C_z(x, y)$ along horizontal slices at various fixed depths z, and of the horizontally-averaged $C(z)$ in a vertical slice between a transmitter and receiver. The method was called ocean acoustic tomography.

* Department of Applied Mathematics and Theoretical Physics, University of Cambridge, Silver Street, Cambridge CB3 9EW, U.K.

† On leave from Scripps Institute of Oceanography, University of California, San Diego, La Jolla, CA 92093, U.S.A.

‡ On leave from Department of Earth and Planetary Sciences, and Department of Meteorology and Physical Oceanography, Massachusetts Institute of Technology, Cambridge, MA 02139, U.S.A.

In the meantime there have been several two-dimensional experiments and one three-dimensional experiment (THE OCEAN TOMOGRAPHY GROUP, 1982). The results support the proposed method as effective for mesoscale problems, and they suggest the application to gyre scales. Given this success, it is now necessary and interesting to explore further the full scope of tomographic methods.

In MW we considered the problems of measuring the field of sound speed $C(x, y, z)$ and its perturbations $\delta C(x, y, z)$, given the acoustic travel times along many different paths. Sound-speed perturbations are largely the result of temperature perturbations $\delta\theta(x, y, z)$, and these can, under normal circumstances, be inferred with useful precision from $\delta C(x, y, z)$. WORCESTER (1977) measured the velocity field $u(x, y, z)$ from the *difference* in travel time in reciprocal transmissions over 25 km. This has opened the possibility of extending such velocity measurements over mesoscales, or, possibly, even gyre scales. An experiment over 300-km ranges will take place in 1982. Hence, we will discuss how the combined measurement of $\delta C(x, y, z)$ and $u(x, y, z)$ would permit a distinction between barotropic and baroclinic perturbations, and further lead to an improvement in vertical resolution as compared to one-way transmissions leading to $\delta C(x, y, z)$ only.

For ease of interpretation, we shall refer most of the discussion to a layered ocean. A better procedure (and one that we use in practice) is based on a continuous x, y, z distribution (CORNUELLE, 1982), with a specified covariance matrix. By choosing layers thick in some regions and thin in others and stating the variance of all those layers, we have likewise specified the covariance matrix (although not in the most efficient form). The result for the layered ocean can then be re-interpreted in terms of a continuous distribution.

The present discussion is in terms of the easily visualized acoustic ray propagation approximation. A more powerful representation in terms of acoustic modes is now being studied, but we believe that the essential conclusions will not be altered. There is a close analogy between ray turning points and mode turning points; it is the vertical spacing of the ray or mode turning points that determines the vertical resolution of long-range acoustic monitoring.

TRAVEL TIME ERRORS

The problem is one of resolution vs precision. The fundamental measurement here is travel time, t, between an acoustic transmitter and receiver. The error bars in the measured δC (and hence $\delta\theta$) and u are proportional to the t error bar.

In our work so far the transmitted pulse width is about 50 ms (THE OCEAN TOMOGRAPHY GROUP, 1982), and this is to be reduced to 10 ms using a broadband source. Over a 1-Mm (1000 km) transmission, which is to serve as standard in this paper, the interference between micromultipaths (associated with internal waves and other fine structure) spreads a given pulse by an incremental 10 ms (J. SPIESBERGER, private communication). The centroid of the broadened pulse can be read to a precision of the pulse width times (signal-to-noise)$^{-\frac{1}{2}}$. For an initial pulse width of 10 ms spread to 20 ms and a 20 dB signal-to-noise ratio (100 to 1 power ratio), the error is then 2 ms. The value can be further reduced by forming averages over many independent measurements. We shall use, slightly optimistically, a standard value of 1 ms. Position keeping of a taut mooring (using bottom transponders) can be to 1 m, corresponding to a time error of 2/3 ms. Clock errors can be kept to about the same limit. Thus, 1 ms serves as a convenient standard of what can be achieved under favourable (but realistic) circumstances.

The fractional error in a $x = 1$ Mm transmission is then r.m.s. $(C\delta t/x) = 1.5 \times 10^{-6}$, and this is proportional to the r.m.s. error in $\delta C/C$ and u/C. The tomographic inversion process magnifies the error for some layers and reduces it for others by a factor α, which is generally of order 1. Accordingly, r.m.s. $(\delta C/C)$ = r.m.s. (u/C) = α r.m.s. $(\delta t/t)$. The temperature coefficient of sound speed is about $a = (\delta C/C)/\delta\theta = 3.2 \times 10^{-3}(°C)^{-1}$, or $3.2 \times 10^{-6}\,(m°C)^{-1}$, and so with $C = 1.5 \times 10^6$ mm s^{-1}

$$\left.\begin{aligned} \text{r.m.s. } (m°C) &= (\alpha/a)\ \text{r.m.s. } (\delta t/t) \approx 0.5\ \alpha, \\ \text{r.m.s. } (\text{mm s}^{-1}) &= \alpha C\ \text{r.m.s. } (\delta t/t) \approx 2.5\ \alpha. \end{aligned}\right\}$$

OCEAN ACOUSTIC AND DYNAMIC WAVE GUIDES

The density stratification [conveniently portrayed by the buoyancy frequency $N = (-g\rho^{-1}\,d\rho/dz)^{\frac{1}{2}}$] diminishes with depth from a typical value of 3 to 10 cycles per hour (cph) in the upper thermocline to 0.25 cph near the deep-sea floor. The decrease is associated with a trapping of energy (internal waves, planetary waves, ...) in the upper ocean. The vertical gradient dC_p/dz of potential (true minus adiabatic) sound speed is similar to $d\rho/dz$. The true sound speed, however, reaches a minimum at some depth (typically 1 km) and then increases downward as a result of the effect of pressure in an increasingly adiabatic ocean. As a result, sound energy is trapped in an interior wave guide and not, as the ocean dynamic energy, in a surface wave guide.*

There is then a mismatch between the shallow dynamic and deep acoustic wave guides, and this is fundamental to the present subject. Consider now a disturbance $\delta C(z)$ or $u(z)$ from some oceanographic feature. Typically, this will be larger in the shallow waters above the sound axis than in the deep waters beneath the axis. The acoustics, on the other hand, are more sensitive to the disturbance beneath the axis (where the ray curvature is small and the ray loops are long). There is then a conflict between ocean dynamics favoring the upper oceans and ocean acoustics favoring the lower oceans. Which is the more important? It turns out that with regard to velocities weighted according to $u \sim N^{\frac{1}{2}}(z)$ the two effects just about balance and a measured disturbance in travel time has comparable contributions from above and beneath the sound axis. But for disturbances in the sound field (i.e., density), the weighting is by $\delta C \sim N^{3/2}(z)$, and here most of the contributions come from the upper oceans (as asserted by MW).

These general comments will now be discussed in detail in the context of five problems: (1) The vertical resolution and associated questions of vertical ambiguity if nothing were known of the measured field. Results apply equally to $\delta C(x, y, z)$ and $u(x, y, z)$. We call this the agnostic case. (2) Improved resolution if we accept $N(z)$ weighting for the measured disturbances. (3) Further improvements if we can take advantage of mode weighting. This is perhaps the most orthodox approach. (By 'modes' we will now always mean oceanographic modes, not acoustic ones.) (4) Constraining imposed by the thermal-wind equation relating the two fields. (5) Separation of the ocean disturbances into barotropic and baroclinic modes.

* In an arctic environment there is no sound-speed minimum and the acoustic energy is in fact trapped in a surface duct.

INVERSE PROBLEM

The observables are the travel-time perturbations $\Delta_{mn} = \delta t_{mn}$ between a source at m and a receiver at n. If source and receiver are co-located, we can refer to the sum and difference of reciprocal travel times:

$$s_i = \tfrac{1}{2}(\Delta_{mn} + \Delta_{nm})/t_0$$
$$d_i = \tfrac{1}{2}(\Delta_{mn} - \Delta_{nm})/t_0 \tag{1}$$

between any station pair $i(m, n)$, $i = 1, 2 \ldots I$. Here t_0 is some mean reference travel time, and s_i, d_i are dimensionless perturbations. The perturbations are considered the consequence of perturbations in sound speed δC_j and of a velocity component* u_j in layer j, $j = 1, 2, \ldots J$.

We introduce the dimensionless perturbations

$$\sigma_j = \delta C_j/C_0, \quad \mu_j = u_j/C_0. \tag{2}$$

[$\sigma(z)$ etc. is a function of z; σ_j etc. is $\sigma(z)$ evaluated in layer j; $\boldsymbol{\sigma}$ is the column vector of components σ_j.]

We wish to estimate $\boldsymbol{\sigma}$, $\boldsymbol{\mu}$ from measurements of $\mathbf{s}$, $\mathbf{d}$. They are related by

$$R\boldsymbol{\sigma} = \mathbf{s}, \quad R\boldsymbol{\mu} = \mathbf{d}, \tag{3}$$

where $R = \{R_{ij}\}$ is the fractional time spent by ray i in layer j. The problem is to invert equations (3) to solve for $\boldsymbol{\sigma}$ and $\boldsymbol{\mu}$. The basic information is contained in the R matrix.

We consider three cases:

	No. of rays	No. of layers	
1. Fine resolution	$I = 6$,	$J = 10$	(underdetermined)
2. Coarse resolution	$I = 6$,	$J = 4$	(overdetermined)
3. Fine resolution	$I = 16$,	$J = 10$	(overdetermined)

There is a conflict between resolution and reliability, as always. The first case, which serves as a standard, portrays the situation for an axial source and receiver separated by 1 Mm (1000 km) in a reference sound channel. There are six principal rays corresponding to 40, 38, 36, 34, 32, and 30 turning points, going from a near-axial to a surface-grazing situation. The turning points of the six rays determine the boundaries of 10 layers (Fig. 1). The resolution is about 100 m near the surface and 500 m in the deep ocean. The case is underdetermined and will not give satisfactory results unless further information is supplied. In the second case, the 10 layers are condensed into just two layers above and two layers beneath the axis. In the third case, we maintain the fine resolution but take advantage of additional rays (with odd numbers of turning points). After a lengthy derivation of the R matrix we return to an interpretation of the results for the three cases.

Ray weighting

For small ray inclinations $\theta(z)$ the ray weighting within a depth interval $z \pm \delta z$ is given by $\delta z/\sin\theta$. From Snell's law

* Because of the small ray inclinations, u can be considered the horizontal component in the direction source to receiver. For the present we ignore the range dependence of δC and u.

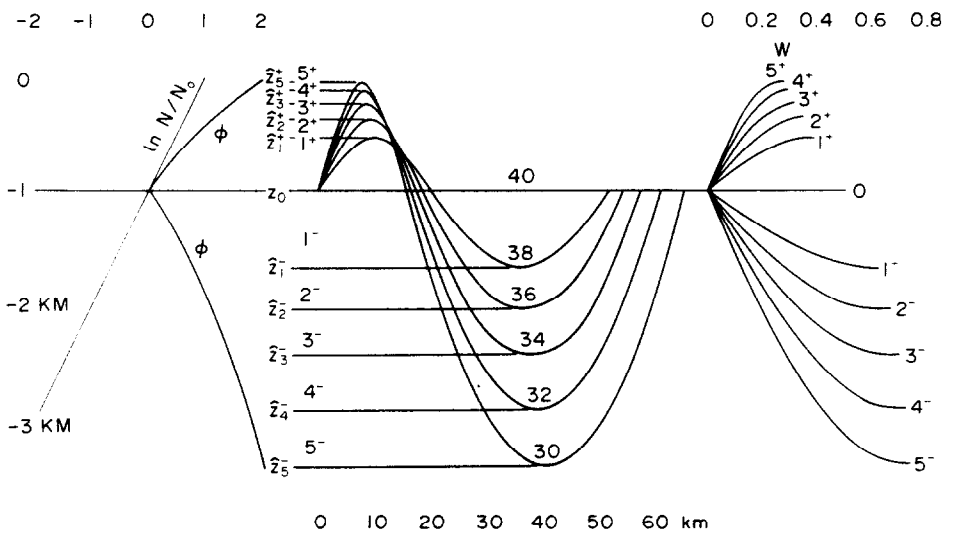

Fig. 1. Left: the reference $N(z)$ and $\phi(z)$ for a stratification scale $B = 1$ km and a sound axis at $z_0 = -1$ km. Middle: Ray diagram for the first convergence zone (taken as $x_{cz} = 50$ km) for an axial transmitter and receiver separated by 1 Mm (1000 km). The turning depths $\hat{z}_0$, $\hat{z}_1^{\pm}, \ldots, \hat{z}_5^{\pm}$ are drawn for $\hat{\phi} = 0$ (axial), 0.79, 1.15, 1.46, 1.73, 2.00 (near surface) corresponding to rays with $p = 40, 38, 36, 34, 32, 30$ turning points. Right: the cumulative ray weighting according to equation (9), with ray i corresponding to turning depths $z_i^{\pm}$. The curves are asymptotically horizontal at the turning depths, associated with the singularity $(1 - C^2(z)/\hat{C}^2)^{-\frac{1}{2}}$ in equation (4). Layers are selected according to turning depths and labelled $j = 1^{\pm}, 2^{\pm}, \ldots, 5^{\pm}$ as shown.

$$\frac{C}{\cos\theta} = \frac{C_0}{\cos\theta_0} = \hat{C},$$

where C_0 and θ_0 refer to the depth of the sound axis z_0, and $\hat{C}$, $\hat{\theta} = 0$ refer to the turning depths $\hat{z}_{\pm}$ above or beneath the axis. Accordingly the weighting is given by

$$w(z)\,\delta z = \frac{(1 - C^2(z)/\hat{C}^2)^{-\frac{1}{2}}\delta z}{\int_{\hat{z}_-}^{\hat{z}_+} dz\,(1 - C^2/\hat{C}^2)^{-\frac{1}{2}}} \tag{4}$$

so normalized that

$$\int_{\hat{z}_-}^{\hat{z}_+} w(z)\,dz = 1.$$

The value $w(z)$ has an integrable singularity at the turning points, and it is more convenient to refer to the cumulative weighting

$$W^{\pm}(z) = \pm \int_{z_0}^{z} w(z)\,dz. \tag{5}$$

Let $\hat{W}^{\pm} = W(\hat{z}_{\pm})$: note that $\hat{W}^{+} + \hat{W}^{-} = 1$.

Model ocean

Some model is needed for $C(z)$. If we can ignore salinity, then $N^2 = -g\rho^{-1}\,d\rho/dz$ is simply related to potential (true minus adiabatic) and true vertical gradients of sound speed:

$$\frac{1}{C}\frac{dC_p}{dz} = \gamma\frac{N^2}{N_0^2}, \quad \frac{1}{C}\frac{dC}{dz} = \gamma\frac{N^2 - N_0^2}{N_0^2} \tag{6}$$

with $\gamma = 1.14 \times 10^{-2}\ \mathrm{km}^{-1}$. The sound speed is a minimum at the axis where $N = N_0$. For a model we use

$$N^2 = N_0^2\ e^{\zeta},\ \zeta = z(z - z_0)/B, \tag{7}$$

which leads at once to the 'reference sound channel' (MUNK, 1974)

$$\frac{C - C_0}{C_0} = B\gamma\phi^2,\ \phi^2 = \frac{N^2}{N_0^2} - \ln\frac{N^2}{N_0^2} - 1. \tag{8}$$

Figure 1 shows a plot of $N(z)$ and $\phi(z)$ for the reference ocean.*

A word of caution is required. The exponential N model is a convenient way to portray the decrease of stratification with depth. But many acoustic effects are sensitive to the details of $C(z)$, and so the present model can only be regarded as an approximation. WUNSCH (1980) studied perturbations to this model.

From (4), (5), and (8) one can get an approximate expression for the cumulative weighting (MW: A13):

$$W^{\pm} = \frac{\dfrac{\eta}{\pi} \pm \dfrac{\sqrt{2}}{3\pi}(1 - \cos\eta)\hat{\phi} + \dfrac{1}{12\pi}(\eta - \cos\eta\sin\eta)\hat{\phi}^2}{1 + \hat{\phi}^2/12} \tag{9}$$

with $\sin\eta = \phi/\hat{\phi}$ and $\hat{\phi} = \phi(\hat{z})$. Depth enters through $\eta\{\phi[N(z)]\}$. The solution applies to small and moderate values of ϕ, and some of our calculations exceed this limitation.

The ray is determined by the turning parameter $\hat{\phi}$. For the simplest case of an axial transmitter and axial receiver separated by a range x, we have (MW: A14):

$$\frac{x}{x_{cz}} = \tfrac{1}{2}(p^+ + p^-) - \frac{\sqrt{2}}{3\pi}(p^+ - p^-)\hat{\phi} + \tfrac{1}{24}(p^+ + p^-)\hat{\phi}^2, \tag{10}$$

where $x_{cz} \approx 50$ km is the convergence zone and where $p^{\pm}$ are the number of upper or lower turning points, $p = p^+ + p^-$. In Fig. 1 we have taken the simplest case of an integer number of double loops, so that $p^+ = p^-$ and $p = 2p^+ = 2p^-$ is an even number. For a given range there are then a finite number of rays starting with the axial ray ($p = 40$, $\hat{\phi} = 0$, $z = z_0$) and ending with an upper turning point just beneath the surface ($p = 30$, $\hat{\phi} = 2.00$, $z_+ = -20$ m). The associated cumulative weighting $W(z)$ is drawn to the right. The slope $dW/dz = w(z)$ is the local weighting, and this becomes infinite (horizontal in the figure) at the turning points. The singularities are most pronounced at the lower turning points.

* This model has sometimes been referred to as the 'canonical' ocean. 'Reference' now seems a more appropriate description.

The slope at the sound axis is

$$\frac{dW}{dz} = \frac{1}{\pi}\frac{d\eta}{dz} = \frac{\sqrt{2}}{\pi}\frac{1}{B\hat{\phi}},$$

and the value at the turning point $\eta = \frac{1}{2}\pi$ is

$$\hat{W}^{\pm} = \tfrac{1}{2} \mp D, \quad D = \frac{(\sqrt{2}/3\pi)\hat{\phi}}{1 + \hat{\phi}^2/12}, \tag{11}$$

so that the lower loops receive greater weight.

The matrix R

Spatial proximity of neighbouring rays is a measure of vertical resolution. The ray-turning depths are widely spaced near the axis (poor resolution) and most closely spaced in the upper ocean (high resolution).* It seems natural to space the layers' boundaries closely together when the resolution is good, and vice versa. We adopt the convention of placing the layer boundaries at the turning depths of integer ray double loops (even p). Thus, layer $1^{\pm}$ extends from z_0 to $z_1^{\pm}$, and layer j^{+} from $z_{j-1}^{\pm}$ to $z_j^{\pm}$, etc. (see Fig. 1).

The weighting of layer $j^{\pm}$ by ray i is then expressed in terms of the cumulative weighting $W^{\pm}(\eta, \hat{\phi})$ in equation (9), according to

$$R_{ij}^{\pm} = W^{\pm}(\eta_{ij}, \hat{\phi}_i) - W^{\pm}(\eta_{i,j-1}, \hat{\phi}_i) \tag{12}$$

with

$$\sin \eta_{ij} = \hat{\phi}_j/\hat{\phi}_i, \ \sin \eta_{i,j-1} = \hat{\phi}_{j-1}/\hat{\phi}_i .$$

$\hat{\phi}_i$ is the value of $\hat{\phi}$ at the turning points of ray i. $\hat{\phi}_{j-1}$ is the value of $\hat{\phi}$ at the boundary nearer the axis of layer j, and $\hat{\phi}_j$ corresponds to the layer boundary further from the axis, or $\hat{\phi}_j = \hat{\phi}_i$, whichever is smaller. (The latter option obtains when the turning point i is within the layer j.)

We need to make an adjustment when p is odd. Thus, $p^{+} = p^{-} + 1$ requires more weight for W^{+} than for W^{-} to allow for the extra upper loop, and *vice versa* when $p^{+} = p^{-} - 1$. This can be done by replacing $W^{\pm}$ in (11) by a modified function

$$W_{\text{mod}}^{\pm} = \frac{p^{\pm}}{\frac{1}{2}(p^{+} + p^{-}) - (p^{+} - p^{-})D} W^{\pm}, \tag{13}$$

where D is defined in (11). This reduces to $W^{\pm}$ when p is even and is normalized so that $\hat{W}_{\text{mod}}^{+} + \hat{W}_{\text{mod}}^{-} = 1$.

THE AGNOSTIC CASE: NO WEIGHTING

Fine resolution with only even loops

The solution with least possible *a priori* prejudice as to its structure is obtained by normalizing all rows of the coefficient matrix to unity and all columns to unity as described by MW and elsewhere. The normalizations correspond in the former case to the assumption that all

* The total number of ray arrivals increases (the resolution improves) linearly with range; however for large ranges, the problem is more conveniently formulated in terms of acoustic normal modes instead of rays.

ray arrivals are determined with equal probable error and in the latter that the necessary perturbations in sound speed are equally likely to occur in any of the layers.

Table 1 shows the matrix R_{ij} for the six rays with integer double loops (p even) only. We begin by using double loops. The 10 layers in Fig. 1 have now been relabeled consecutively and appear from left to right to correspond to the usual matrix format. Depth limits are indicated. The zeros correspond to layers beyond the turning points. The weighting is relatively heavy at the turning points, particularly for the lower turning point of the steep rays, but the weighting is by no means singular. The axial layers are relatively heavily weighted because they are so thick.

We now return to equations (3). The problem is to solve for σ (or μ) as a weighted sum of the measurements $\mathbf{s}$ (or $\mathbf{d}$). The procedure to be followed (WUNSCH, 1978; MW) is to determine the eigenvectors $\mathbf{U}_k$, $\mathbf{V}_k$ according to

$$RR^T\mathbf{U}_k = \lambda_k^2\mathbf{U}_k,\ R^TR\mathbf{V}_k = \lambda_k^2\mathbf{V}_k, \tag{14}$$

where λ_k^2 are the eigenvalues. Equations (14) have non-zero solutions (the singular values) λ_k, $k = 1, K$. The solutions are ordered starting with the largest λ_k. For each singular value λ_k there is an ordered data set

$$S_k = \sum_{i=1}^{I} U_{ki}s_i,\ k = 1, K, \tag{15}$$

with $K(\leqslant I)$ independent pieces of information, derived as a linear weighted sum of the measured data set s_i, $i = 1, I$. If the data set s_i does not consist of I independent observations, then the rank K will be less than the dimension I of s_i. In the present case $\lambda_k^2 = 5.0, 2.0, 1.3, 1.0, 0.8$, and 0.2. The smallness of λ_6 indicates that the data set may not be quite of rank six: the rays may not give completely independent information. Whether we can use five or six equations depends then on the precision of the measurements (as will be shown).

Table 1. *The weight matrix* R_{ij} *for fine resolution with only even loops*

		Previous layer designation									
		5^-	4^-	3^-	2^-	1^-	1^+	2^+	3^+	4^+	5^+
		z in meters									
		−3460	−2960	−2470	−2060	−1700	−1000	−530	−350	−210	−100	−20
		Layer No. j									
No. of loops p	Ray No. i	1 Deep	2	3	4	5	6	7	8	9	10 Shallow
40 (Axial)	1	0	0	0	0	0.50	0.50	0	0	0	0
38	2	0	0	0	0	0.61	0.39	0	0	0	0
36	3	0	0	0	0.39	0.27	0.17	0.17	0	0	0
34	4	0	0	0.36	0.13	0.19	0.12	0.08	0.12	0	0
32	5	0	0.34	0.13	0.09	0.15	0.10	0.04	0.07	0.08	0
30 (Steep)	6	0.32	0.12	0.10	0.06	0.12	0.08	0.04	0.03	0.05	0.08

The first two (of six) eigenvectors $\mathbf{U}_k$ have the components

	Ray$_i$					
	1 (Axial)	2	3	4	5	6 (Steep)
U_{1i}	+0.17	+0.16	+0.35	+0.46	+0.54	+0.57
U_{2i}	−0.26	−0.25	−0.52	−0.38	+0.10	+0.67

Thus, S_1 is the travel-time perturbation averaged over all rays (with greater weighting given to steep rays), and S_2 is the perturbation of steep rays minus that of flat rays.

The ordered data set S_k can be written as a weighted sum of contributions from the perturbations σ_j in layer j:

$$S_k = \sum_{j=1}^{J} V_{jk}\sigma_j . \tag{16}$$

The first two-layer eigenvectors $\mathbf{V}_k$ have the components

	Layer									
	1 (Deep)	2	3	4	5	6	7	8	9	10 (Shallow)
V_{1j}	0.26	0.32	0.34	0.32	0.32	0.29	0.34	0.36	0.34	0.26
V_{2j}	0.48	0.24	−0.08	−0.31	−0.30	−0.29	−0.29	−0.07	0.33	0.48

As expected, all layers contribute fairly equally to the ray-averaged perturbation S_1, whereas the steep minus flat ray perturbation S_2 arises (not surprisingly) from the difference of the σ_j in the deep and shallow layers minus the σ_j in the axial layers.

The solution is written

$$\sigma_j = \sum_{k=1}^{K} \left\{ \frac{\sum_{i=1}^{I} U_{ik} s_i}{\lambda_k} \right\} V_{jk} \tag{17}$$

or simply

$$\boldsymbol{\sigma} = \sum_{k=1}^{K} \frac{\mathbf{U}_k^T \mathbf{s}}{\lambda_k} \mathbf{V}_k .$$

A resolution test is as follows: suppose a unit disturbance is placed into the deepest layer ($j = 1$) and no disturbance elsewhere: $\sigma_j = \delta_{1j}$. We then solve the forward problem $s_i = \Sigma_j R_{ij}\sigma_j = R_{i1}$ and evaluate σ_j from (17). It can be shown that the result equals column 1 of VV^T (where V is the matrix whose columns are $\mathbf{V}_k$, $k = 1, K$) and writing the column of VV^T across rather than down.

Col. (VV^T)	Layer j 1 (Deep)	2	3	4	5	6	7	8	9	10 (Shallow)
1	0.49	−0.05	0.03	−0.02	0	0	0.02	−0.03	0.07	0.49
2	−0.05	0.56	−0.06	0.02	0	0	−0.02	0.07	0.48	−0.05
5	0	0	0	0	1.00	0	0	0	0	0
6	0	0	0	0	0	1.00	0	0	0	0
9	0.07	0.48	−0.05	0.01	0	0	−0.01	0.05	0.45	0.07
10	0.49	−0.05	0.03	−0.02	0	0	0.02	−0.03	0.07	0.49

Ideally the first number in column 1 should be 1 and the rest zero. In fact, the first and last numbers are each about $\frac{1}{2}$, so that a disturbance in the deepest layer has been improperly apportioned between the deepest and shallowest layers. More generally an attempt to resolve unity in layer j with zero everywhere else is represented by column j of VV^T; thus VV^T is 'the resolution' matrix. Ideally VV^T should be a unit diagonal matrix; instead, we find an up–down ambiguity between conjugate layers (with equal sound speed). Only a disturbance in one of the two axial layers gives the desired results. The diagonal terms (which should everywhere be unity) are in fact Diag. $(VV^T) = 0.49$ (Deep), 0.56, 0.55, 0.54, 1.00, 1.00, 0.47, 0.47, 0.45, and 0.49 (Shallow). The results are good near the axis and unacceptable elsewhere.

The interpretation of UU^T is more difficult (with U the matrix whose columns are $\mathbf{U}_k$, $k = 1, K$). A unity diagonal element i means that the information contained in ray i is completely independent of all other measured rays and that the information has been used completely in determining the solution. If the diagonal element is less than unity and there are non-zero off-diagonal elements in column i, then the information contained in ray i is linearly dependent upon that contained in those rays to which the non-zero off-diagonal elements correspond. The sum of the diagonal elements equals the rank of the system. For the present case of six rays and 10 layers, where the rank of the system is chosen to be six, then the UU^T matrix is of necessity the identity matrix, and all rays contribute fully to the solution.

The above result can be stated from the converse point of view. If a diagonal element of UU^T is unity, then the information available about the system is adequate to make changes in the layer perturbations σ_j, $j = 1, J$, such that only ray i is affected. If the diagonal element is not unity, then one is justified in making changes only such that the corresponding linear combination of rays given by row i $[UU^T]\mathbf{s}$ is affected.

We require an estimate of the experimental errors in the computed fractional sound speed σ and velocity μ arising from the error in measuring travel time. This is obtained from

$$\text{r.m.s. } (\sigma_j) = \alpha_j \text{ r.m.s. } (\mathbf{s}),\ \text{r.m.s. } (\mu_j) = \alpha_j \text{ r.m.s. } (\mathbf{d}),$$

with

$$\alpha_j^2 = \sum_{k=1}^{K} V_{jk}^2 / \lambda_k^2 . \tag{18}$$

The results are $\alpha_j = 0.5$ (Deep), 0.6, 0.6, 0.6, 2.9, 3.6, 1.1, 1.4, 1.8, and 2.0 (Shallow). We shall set r.m.s. (s) = r.m.s. $(d) = 1.5 \times 10^{-6}$ for a travel-time error of 1 ms, thus leading to a temperature error of 0.5 α_j m °C and a current error of 2.5 α_j mm s^{-1} (equation 1).

The worst result is in layer 6: 1.8 m°C and 9 mm s^{-1}, respectively. This is acceptable. We have allowed for the fact that for an even number of turning points there are two rays (upward and downward at a source) so that the r.m.s. error is reduced by $\sqrt{2}$. The conclusion is that the underdetermined case of six rays in 10 layers fails on account of an up–down ambiguity in conjugate layers. We will show that the ambiguity can be resolved by including in the analysis some dynamic constraints. At the moment we want to see how far we can go without imposing preconceived ideas.

Coarse resolution with only even loops

We now collapse the 10 layers into four (Table 2). This corresponds roughly to a consideration of the lowest two baroclinic modes, so this is perhaps the crudest ocean model one should consider.

The case is now overdetermined with the eigenvalues $\lambda_k^2 = 2.9$, 1.1, 0.03, and 0.001. Accordingly with rank four, the first two sums of the data set carry most of the information. The UU^T diagonal element tells us that all rays contribute significantly to the results, though the shallowest and steepest are the most important.

	Ray i					
	1 (Axial)	2	3	4	5	6 (Steep)
Diag. (UU^T)	0.94	0.37	0.68	0.66	0.42	0.93

The sum of diagonals equals four, the rank of this inversion.

The first two ray eigenvectors $\mathbf{U}_k$ and layer eigenvectors $\mathbf{V}_k$ have the same qualitative features as in the preceding 10-layer case, with $k = 1$ representing a fairly straight average

Table 2. The weight matrix R_{ij} for coarse resolution with only even loops

		Previous layer designation			
		$5^-, 4^-, 3^-$	$2^-, 1^-$	$1^+, 2^+$	$3^+, 4^+, 5^+$
		z in meters			
		−3460	−2060	−1000	−350	−20
				Layer No. j		
No. of loops p	Ray No. i	1 Deep		2	3	4 Shallow
40 (Axial)	1	0		0.50	0.50	0
38	2	0		0.61	0.39	0
36	3	0		0.66	0.34	0
34	4	0.36		0.32	0.20	0.12
32	5	0.47		0.24	0.14	0.15
30 (Steep)	6	0.54		0.18	0.12	0.16

over all rays with quite even contributions from all layers and $k = 2$ representing a difference steep minus flat rays associated with outlying minus axial layers.

The important change from the previous case is that the diagonal elements of VV^T are now 1, as they must be in a full-rank overdetermined case. The evaluation depends therefore on an analysis of the layer error bars for a given experimental error in travel time (here 1 ms). The results are shown below.

	Layer j			
	1 (Deep)	2	3	4 (Shallow)
α_j	11	1.8	2.6	35
r.m.s. (mC°)	5	0.9	1.3	18
r.m.s. (mm s^{-1})	25	5	6	88

The worst error is in the upper layers, but even there the temperature error is an acceptable 0.02°C. The velocities are usefully measured in all but the upper layers. Still this crude model would yield useful results.

Fine resolution with even and odd loops

So far the analysis has been for even values of p; does the additional information contained in rays with odd p values permit an adequate determination of the 10-layer case? Each ray group consists of four constituents. For example, group 38 consists of 39^+, 39^-, 38^+, 38^-. Here $38^\pm$ refers to rays going up or down at the source, each with 19 double loops; $39^\pm$ has 19 double loops plus an extra upper or lower loop. We have weighted even loops by $\sqrt{2}$ relative to odd loops to account for the fact that they consist of an upward plus a downward ray: we do not account for the generally different overall amplitudes of the arriving ray sequence.

Table 3 gives the weight matrix. The rays associated with $p = 40, 38, \ldots 30$ are the ones considered in Table 1. The 10 eigenvalues λ_k^2 are 5.4, 1.9, 1.2, 0.87, 0.70, 1×10^{-2}, 3×10^{-3}, 2×10^{-3}, 4×10^{-4}, and 5×10^{-5}. There is a break between the first five and the five remaining values, so there are still only five large eigenvalues as in the previous case of only even p. Thus, the addition of odd loops can only lead to a moderate improvement of the 10-layer case. The diagonal elements of UU^T going from $i = 1$ (axial ray) to $i = 16$ (steep ray) are 0.95, 0.17, 0.13, 0.70, 0.18, 0.26, 0.73, 0.14, 0.48, 0.71, 0.39, 0.36, 0.72, 0.84, 0.43, and 0.83. The underlined values correspond to even loop arrivals, showing (as anticipated from the differential weighting) that these rays dominate (but not overwhelm) the inversion process.

The first two components, $\mathbf{U}_k$ and $\mathbf{V}_k$, have the same general character as for the standard case of only even p. For this standard case, we previously found

Diag. $VV^T = 0.49$	0.56	0.55	0.54	1.00	1.00	0.47	0.47	0.45	0.49
Error $\alpha_j = 0.49$	0.58	0.57	0.62	2.9	3.6	1.1	1.4	1.8	2.0
Deep									Shallow

with up–down ambiguity for all but the axial layers. Including the odd terms, but using only the first six terms of the ordered data set δ_k (for ready comparison with above),

Diag. $VV^T = 0.50$	0.50	0.51	0.50	1.00	1.00	0.50	0.49	0.50	0.50
Error $\alpha_j = 0.35$	0.36	0.38	0.38	2.2	2.9	1.0	1.1	1.2	1.2

Table 3. The weight matrix R_{ij} for fine resolution with even and odd loops

No. of loops p*	Ray No. i	Layer No. j 1 Deep	2	3	4	5	6	7	8	9	10 Shallow
40 (Axial)	1	0				0.50	0.50				
39+	2					0.59	0.41				
39−	3					0.57	0.43				
38	4					0.61	0.39				
37+	5				0.27	0.38	0.24	0.12			
37−	6				0.33	0.31	0.22	0.15			
36	7				0.39	0.27	0.18	0.16			
35+	8			0.22	0.22	0.24	0.15	0.09	0.08		
35−	9			0.29	0.17	0.21	0.15	0.08	0.11		
34	10			0.35	0.15	0.19	0.13	0.06	0.12		
33+	11		0.18	0.21	0.13	0.18	0.12	0.05	0.07	0.06	
33−	12		0.27	0.15	0.11	0.16	0.11	0.05	0.06	0.09	
32	13		0.32	0.13	0.10	0.15	0.10	0.05	0.05	0.10	
31+	14	0.18	0.19	0.12	0.10	0.14	0.09	0.04	0.04	0.05	0.05
31−	15	0.27	0.13	0.10	0.08	0.12	0.09	0.04	0.04	0.04	0.08
30 (Steep)	16	0.31	0.12	0.09	0.08	0.12	0.08	0.03	0.03	0.04	0.09

* p^+ means upwards at source.

The error bars are only moderately reduced, and the up–down ambiguity remains. But the interesting improvement comes with additional terms in the ordered data set. For example, extending the above summation $k = 1, 6$ to $k = 1, 8$ gives

Diag. VV^T =	0.52	0.97	0.70	0.82	1.00	1.00	0.81	0.70	0.97	0.52
Error α_j =	1.9	9.0	4.6	5.8	2.2	2.9	13.7	13.5	28.7	7.0

Thus, the resolution is improved for all but the lowest and uppermost layer, at the expense of an enhanced but still acceptable error bar. For the entire data set $k = 1, 10$, the diagonals are all unity (as they must be for an overdetermined system), but the errors are now forbidding: error $\alpha_j = 63$, 15, 15, 14, 2.3, 2.9, 33, 44, 46, and 216.

Our conclusion is that the inclusion of odd loops can lead to a significant improvement in resolution, but there remains an up–down ambiguity with regard to the very shallow and very deep ocean. (We must repeat that we have yet to make use of our *a priori* knowledge of ocean dynamics.)

N WEIGHTING

The discussion so far has dealt with the 'agnostic' inversion (the 'naive' inversion of MW). But we now wish to impose our previous knowledge of the ocean variability on the inversion. This leads to a virtual elimination of the up–down ambiguity but with the danger that we may misinterpret some unexpected ocean disturbances.* The inversion process does, however, provide some safeguards that warn if the imposed constraints are grossly inconsistent with the data.

* An example could be a bottom-trapped wave. Another example is provided in the climatological context where we have no *a priori* information of how such disturbances are weighted with depth.

σ and μ weighting

The two 'measured' quantities are

$$\sigma(z) = \frac{\delta C_{\text{pot}}}{C} = \frac{1}{C}\frac{dC_{\text{pot}}}{d\rho}\frac{d\rho}{dz}\xi = \frac{\alpha}{g}N^2\xi$$

$$\mu = u/C,$$

where ξ is vertical displacement and $\alpha = (\rho/C)(dC/d\rho) \approx 25$.

It is convenient to write the velocity as a sum of two parts: $u = u_0 + u_j$, $\mu = \mu_0 + \mu_j$, where u_0 is the barotropic component, and u_j is the baroclinic component in layer j. The calculation of the barotropic component is discussed later. For now we write simply u for u_j.

WKBJ scaling gives $\xi \sim N^{-\frac{1}{2}}$, $u \sim N^{+\frac{1}{2}}$, hence

$$\sigma(z) \sim N^{\frac{1}{2}}(z),\ \mu(z) \sim N^{\frac{1}{2}}(z). \tag{19}$$

Following MW, the expectation that the disturbances have this vertical amplitude distribution is introduced into equations (3) by rewriting them as

$$RA^{\frac{1}{2}}A^{-\frac{1}{2}}\boldsymbol{\sigma} = \mathbf{s},\ RB^{\frac{1}{2}}B^{-\frac{1}{2}}\boldsymbol{\mu} = \mathbf{d}$$

or

$$R'\boldsymbol{\sigma}' = \mathbf{s},\ R''\boldsymbol{\mu}' = \mathbf{d}$$

$$R' = RA^{\frac{1}{2}},\ \boldsymbol{\sigma}' = A^{-\frac{1}{2}}\boldsymbol{\sigma},\ R'' = RB^{\frac{1}{2}},\ \boldsymbol{\mu}' = B^{-\frac{1}{2}}\boldsymbol{\mu},$$

where $A^{\frac{1}{2}}$ and $B^{\frac{1}{2}}$ are diagonal matrices whose elements $A^{\frac{1}{2}}_{ii}$ and $B^{\frac{1}{2}}_{ii}$ are $N^{\frac{1}{2}}$ and $N^{\frac{1}{2}}$, respectively, evaluated in layer i (more generally, A and B are the *a priori* covariance matrices of the solutions $\boldsymbol{\sigma}$, $\boldsymbol{\mu}$). One proceeds as before but using the new variables $\boldsymbol{\sigma}'$, $\boldsymbol{\mu}'$ and solving at the end for $\boldsymbol{\sigma}$, $\boldsymbol{\mu}$. R', R'' can be evaluated from R by finding the modification to the weight $w(z)$ when it is multiplied by the appropriate vertical scaling function in $A^{\frac{1}{2}}$, $B^{\frac{1}{2}}$.

The contribution of $\sigma(z)$ weighted by $w(z) = dW/dz$ between the axis and some depth z is now proportional to

$$\int_{z_0}^{z} N^{\frac{1}{2}}(z')\,w(z')dz' = \int_0^{W(z)} N^{\frac{1}{2}}\,dW$$

$$= N^{\frac{1}{2}}(z)W^{\pm}(z) - \frac{3}{2}\int_{N_0}^{N(z)} W^{\pm}N^{\frac{1}{2}}\,dN \tag{20}$$

and similarly for $\mu(z)$

$$\int_{z_0}^{z} N^{\frac{1}{2}}(z')\,w(z')\,dz' = N^{\frac{1}{2}}(z)W^{\pm}(z) - \frac{1}{2}\int_{N_0}^{N(z)} W^{\pm}N^{-\frac{1}{2}}dN. \tag{21}$$

The use of N as an independent variable is a convenient way of evaluating the turning point singularities.

The cumulative contributions are drawn in Fig. 2 for a typical ray ($\hat{\phi} = 1$) and a steep near-surface ray ($\hat{\phi} = 2$). The major contribution to σ comes from the upper ocean, especially for

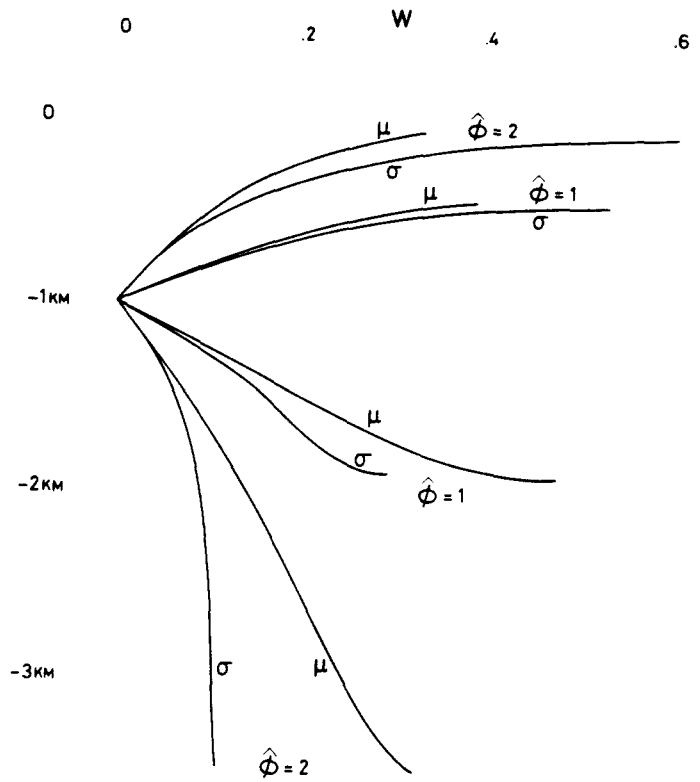

Fig. 2. The cumulative contribution of WKBJ weighted perturbation in sound speed (σ) and velocity (μ) to the perturbations in travel time. $\hat{\phi} = 1$ corresponds to a moderately inclined ray and $\hat{\phi} = 2$ to a steep near-surface ray.

steep rays: dynamic weighting dominates over acoustic weighting. The situation is reversed for μ at $\hat{\phi} = 1$; most of the contribution comes from the lower ocean and acoustic weighting (which favours the lower ocean) dominates over dynamic weighting (which favours the upper ocean).

Fine resolution with only even loops

We recall the previous result for the standard (unweighted) case of 10 layers and six even-loop arrivals:

Diag. VV^T =	0.49	0.56	0.55	0.54	1.00	1.00	0.47	0.47	0.45	0.49
Error α_j =	0.49	0.58	0.57	0.62	2.9	3.6	1.1	1.4	1.8	2.0
	Deep									Shallow

With WKBJ weighting $\sigma \sim N^{\frac{1}{2}}$,

Diag. VV^T =	0	0	0	0.02	1.00	1.00	0.99	1.00	1.00	1.00
Error α_j =	0	0	0	0.02	2.9	3.6	2.6	3.1	4.5	4.4

The resolution in the upper ocean is now nearly perfect (consistent with the MW result for similar first-mode weighting), at the expense of only moderately increased error bars. But a

disturbance confined to the deep water would not be properly identified—it would be misplaced above the sound axis.

WKBJ weighting for velocity $\mu \sim N^{\frac{1}{2}}$ is less dominated by the upper ocean. The result is:

Diag. VV^T =	0.04	0.09	0.15	0.22	1.00	1.00	0.79	0.86	0.91	0.95
Error α_j =	0.04	0.10	0.16	0.26	2.9	3.6	2.0	2.6	4.0	4.1

The upper layers are still not fully resolved.

THE ORTHODOX CASE: MODE WEIGHTING

The preceding N weighting is, strictly speaking, most appropriate if the mesoscale is a sum of a fairly large number of high modes. Over much of the ocean, a low mode dominance is a better description (THE MODE GROUP, 1978). MW used a vertical weighting appropriate to the lowest linear baroclinic mode. N weighting is probably more appropriate in some ocean areas and can sensibly be regarded as mid-way between the agnostic and the orthodox approach.

We have applied the N weighting because the solutions are quite insensitive to the numerical details (MW showed that the second baroclinic mode could be correctly obtained even when the weighting appropriate to the lowest mode was imposed) and indeed the shape of the first baroclinic density and velocity mode is not far from $N^{\frac{1}{2}}$. If one wishes to use normal modes, then our resolution and various estimates are better expressed in mode space. not in physical layer space. This is not pursued here, as the layered ocean model is simpler to interpret. However, the poor resolution in the deep ocean for the layered model is unnecessarily pessimistic where the normal mode approach is appropriate.

A full mode weighting would impose a correlation structure on the layers as well as a variance, a procedure that can be carried out in straightforward fashion using covariance matrices. The correlations provide even more information to the inversion and should be used where appropriate.

If the normal modes are to be used rigorously, they should be computed in the presence of the background mean shear. One can formulate the inversion in such a way that the mean shear is determined as part of the inversion, as well as the mode shapes, in what then becomes, potentially, a non-linear inverse problem.

Generally speaking, there is no single best approach and no substitute for the investigator using his judgement about the most relevant physics in a particular experiment.

THERMAL WIND

The discussion so far has dealt with sound speed and particle velocity as two independent fields to be determined by independent measurements according to the two equations (3), but the two fields are not unrelated. Perturbations in sound speed are closely associated with density perturbations, and these are related geostrophically to the flow field. How much is to be gained in a combined analysis of the two fields that takes this relation explicitly into account?

We start with the thermal-wind equations

$$\frac{\partial v}{\partial z} = \frac{g}{\rho f}\frac{\partial \rho}{\partial x}, \quad \frac{\partial u}{\partial z} = -\frac{g}{\rho f}\frac{\partial \rho}{\partial y}. \tag{22}$$

For the present purpose we assume that δc and $\delta\rho$ are uniquely related, thus ignoring the T–S variations. From (6)

$$\delta c = \frac{\partial C_{\text{pot}}}{\partial z}\xi = \frac{C\gamma N^2}{N_0^2}\xi$$

$$\delta\rho = \frac{\partial \rho_{\text{pot}}}{\partial z}\xi = \frac{\rho N^2}{g}\xi = \frac{\rho}{g}\frac{N_0^2}{\gamma}\frac{\delta C}{C}$$

and so (22) can be written in our 'tomographic variables' $\mu = u/C$, $\nu = v/C$, $\sigma = \delta C/C$, in the form

$$\frac{\partial \nu}{\partial z} = q\frac{\partial \sigma}{\partial x}, \frac{\partial \mu}{\partial z} = -q\frac{\partial \sigma}{\partial y}, \tag{23}$$

with

$$q = \frac{N_0^2}{\gamma C f} \approx 2.5.$$

We shall use only the y-components. For computational purposes we re-scale as follows

$$\mu^* = \mu N_0/f,\ \mathrm{d}^* = \mathrm{d}N_0/f,\ y^* = yf/N_0.$$

Then from (3) and (23)

$$\frac{\partial \mu^*}{\partial z} = -q\frac{\partial \sigma}{\partial y^*};\quad R\boldsymbol{\sigma} = \mathbf{s},\quad R\boldsymbol{\mu}^* = \mathbf{d}^*.$$

We envision an experiment consisting of two tomography arrays (to be designated by superscripts N and S (but not to be confused with the buoyancy frequency N) separated by a distance Δy (Fig. 3). The thermal-wind equation in finite difference can now be written

$$\delta_y(\boldsymbol{\sigma}) = D\,\delta_z\boldsymbol{\mu}^*, \tag{24}$$

where

$$\delta_y(\boldsymbol{\sigma}) = \tfrac{1}{2}(\sigma_j^N - \sigma_j^S + \sigma_{j+1}^N - \sigma_{j+1}^S) \tag{25}$$

is the north-to-south difference in δ averaged over the adjoining layers j and $j+1$, and

$$\delta_z(\boldsymbol{\mu}^*) = \tfrac{1}{2}(\mu_{j+1}^{*S} - \mu_j^{*S} + \mu_{j+1}^{*N} - \mu_j^{*N}) \tag{26}$$

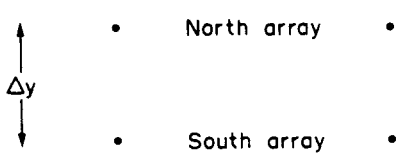

Fig. 3. A two-dimensional array consisting of a north and south station pair. Each station consists of a co-located transmitter and receiver.

is the up–down difference in μ_j^* between adjoining layers, averaged over the S and N arrays. It can be shown that

$$D_j = \frac{D_0}{\delta z_j / B}, \quad D_0 = -\frac{\delta y f / N_0}{Bq} = -0.83,$$

where δz_j is the distance between the centers of layers j and $j+1$. The numerical value is for $\delta y = 50$ km, $f = 1$ cpd, $N_0 = 24$ cpd, $B = 1$ km, $q = 2.5$, and for

$$\delta z = \frac{24Bx/x_{cz}}{p^2} \approx \frac{10B}{x/x_{cz}} \approx \frac{1}{2}B = \frac{1}{2}\text{km},$$

which is the interval between layers at great depth for large x/x_{cz}.

First we take the case of zero barotropic current. We do a grand inversion for the four fields μ_N^*, μ_S^*, σ_N, σ_S at each of 10 depths for a total of 40 unknowns. There are the usual two equations (3) $R\sigma = \mathbf{s}$, $R\mu^* = \mathbf{d}^*$ for each of the six rays at each of the two arrays, with nine additional equations from the thermal-wind equation, for a total of $2 \times 6 \times 2 + 9 = 33$ equations. The rank was found to be 32, so that there are 32 independent equations. The system is still underdetermined.

Without the thermal-wind equation, we have the previous result for 10 layers and six even-looped arrivals:

Diag. $VV^T = 0.49$	0.56	0.55	0.54	1.00	1.00	0.47	0.47	0.45	0.49
Error $\alpha_j = 0.49$	0.58	0.57	0.62	2.9	3.6	1.1	1.4	1.8	2.0
Deep									Shallow

With thermal wind, this becomes

Diag. $VV^T = 0.92$	0.94	0.91	0.88	1.00	1.00	0.63	0.60	0.55	0.58
Error $\alpha_j = 1.1$	1.1	1.3	1.8	2.9	3.6	3.2	4.1	4.6	5.0

for σ (temperature), whereas for μ (current)

Diag. $VV^T = 0.74$	0.78	0.77	0.78	1.00	1.00	0.73	0.73	0.72	0.75
Error $\alpha_j = 4.4$	3.8	3.4	1.8	2.3	2.8	4.4	10.2	14.1	15.7

So the resolution has improved considerably, particularly for the deep ocean and for temperature, at the expense of increased (but generally acceptable) error bars. This is for the agnostic case. When N weighting is introduced, then for the standard case of 10 layers and six even-looped arrivals with $N^{\frac{1}{2}}$ weighting for σ (temperature)

Diag. $VV^T = 0$	0	0	0.02	1.00	1.00	0.99	1.00	1.00	1.00
Error $\alpha_j = 0$	0	0	0.02	2.9	3.6	2.6	3.1	4.5	4.4

without the thermal-wind equation, but with thermal wind

Diag. $VV^T = 0.50$	0.50	0.51	0.52	1.00	1.00	0.98	0.99	1.0	1.0
Error $\alpha_j = 0.88$	0.92	1.1	1.7	2.9	3.6	3.6	4.6	5.6	5.9

Similarly with $N^{\frac{1}{2}}$ weighting for μ (current)

Diag. VV^T =	0.04	0.09	0.15	0.22	1.00	1.00	0.79	0.86	0.91	0.95
Error α_j =	0.04	0.10	0.16	0.26	2.9	3.6	2.0	2.6	4.0	4.1

without the thermal-wind equation, but with thermal wind

Diag. VV^T =	0.52	0.55	0.57	0.61	1.00	1.00	0.89	0.93	0.95	0.98
Error α_j =	4.4	3.8	3.4	1.8	2.3	2.8	4.5	10	14	16

The upper-ocean resolution for current has improved and there is now good resolution for both temperature and current. The dramatic improvement is in the lower ocean, where we previously had no information and where the thermal-wind equation now provides useful (but still limited) information.

The above use of the thermal-wind equation provides an example of the improvement in the inversions from the application of a dynamical constraint. Linear vorticity dynamics, e.g., the beta spiral (SCHOTT and STOMMEL, 1978) provides further possible constraints.

BAROTROPIC CURRENT

It has been traditional to distinguish that part (baroclinic) of the current peculiar to stratified fluids from that (barotropic) which could be sustained also in a homogeneous fluid. But there is no uniquely defined distinction, and the need for a specific procedure makes the ambiguity explicit.

There are at least three conventional definitions for the barotropic current: (1) $\mu_0 = \mu_0'$ is the vertically-averaged current. With linear Rossby-wave dynamics over a flat bottom, this definition emerges as the lowest (0th) mode; (2) $\mu_0 = \mu_0''$ is the current field associated with the horizontal gradient in the *total* mass of the water column above the bottom, whereas the remaining baroclinic flow is due to interior density gradients (local heating and cooling). This is the definition used by FOFONOFF (1962). Because the baroclinic current then vanishes at the lower boundary, it is clear that μ_0'' equals the bottom velocity. (3) $\mu_0 = \mu_0'''$ is some arbitrary constant added to the thermal wind (itself subject to an arbitrary integration constant) to satisfy additional constraints. This could be to make the total current vanish at some preconceived 'depth of no motion' or to satisfy some mass conservation equations (as used in the 'geostrophic inversion' of WUNSCH, 1978); or, as here, to satisfy some acoustic constraints.

We shall make some estimates for case (3). The other two cases easily follow from μ_0' = weighted mean of $(\mu_0''' + \mu_j)$ and $\mu_0'' = \mu_0''' + \mu_1$.

The modification to the preceding thermal-wind inversion is simple. Write $\mu_0^* + \mu_j^*$ for the sum of barotropic plus baroclinic currents, so that the previous equation $\sum_j R_{ij}\mu_j^* = d_i^*$ is replaced by $\sum_j R_{ij}(\mu_0^* + \mu_j^*) = d_i^*$. The equation $\sum_j R_{ij}\sigma_j = s_i$ and the thermal-wind equation are unchanged. For the standard 10-layer case, the rank of the system remains at 32, but the number of unknowns is increased from 40 to 42 with the addition of μ_0^N and μ_0^S. The $N^{\frac{1}{2}}$ weighting applies only to the baroclinic component. For the depth-independent barotropic component we choose an *a priori* variance equal to that of μ_{10}, the upper and most energetic baroclinic layer. The result is shown overleaf.

In comparison with our previous result for $\mu_0 = 0$, the resolution is unchanged for $\boldsymbol{\sigma}$ and slightly reduced for the baroclinic $\boldsymbol{\mu}$, and the errors are a bit higher. The barotropic velocity is not well resolved and has a comparatively small error. Examination of the full VV^T matrix shows the barotropic velocities to be strongly dependent on the baroclinic velocities. The result is consistent with what we know to be true—that the barotropic velocity is determined primarily as a residual of the baroclinic velocity.

		Layer j									
σ (Temperature)	0 (Barotropic)	1 (Deep)	2	3	4	5	6	7	8	9	10 (Shallow)
Diag. VV^T		0.50	0.50	0.51	0.52	1.0	1.0	0.98	0.99	1.0	1.0
Error α_j		0.98	0.98	1.2	1.8	2.9	3.6	3.7	4.8	5.9	6.4
μ (Current)											
Diag. VV^T	0.60	0.43	0.47	0.52	0.57	0.81	0.93	0.85	0.91	0.94	0.97
Error α_j	1.7	3.0	2.3	2.4	3.1	3.5	5.3	6.4	13	18	20

We can make the alternative definitions of $\mu_0 = \mu'_0$ and μ''_0 part of the inversion equations and thus automatically obtain resolution and variances. We obtained 0.99 and 0.84 for the resolution and α_j of μ'_0, and 0.64 and 4.5 for μ''_0. (Determination of these additional parameters necessarily slightly changes the resolution and variance of the original unknowns.)

The thermal-wind equation helps only indirectly in the determination of the barotropic current (which has no shear), but there are remedies. Higher-order constraints (e.g., the beta spiral) provide a relationship between absolute velocity and slopes of density surfaces, and this can be used to constrain (and thus improve) the inversion procedure leading to the barotropic component. We defer this consideration until such time that real data can be used.

DISCUSSION

Table 4 gives a summary of the resolution and error bars. These are conflicting requirements; models that improve the resolution also bring up the error bars.

Table 4. ***Representative values of*** *{**resolution**/*r.m.s. *error**} for temperature*** θ *(in* m° C*) and velocity* u *(in* mm s^{-1}*) for a* 1-Mm *range, taking* r.m.s. *(travel time error)* = 1 ms. *Unity corresponds to perfect resolution.* I *is the number of rays and* J *is the number of layers. Layer thickness at various ocean depths is indicated.* K *is the rank and equals* I *unless otherwise stated*

	Case			Agnostic		N weighted	
				θ (m° C)	u (mm s^{-1})	θ (m° C)	u (mm s^{-1})
1a	Even loops only	Fine resolution (m)					
	$I = 6, J = 10$	Upper	100	0.5/0.8	0.5/4	1/2	0.9/7
		Axial	600	1/1.6	1/8	1/1.6	1/8
		Deep	500	0.5/0.3	0.5/1.5	0/	0.1/
2	Even loops only	Coarse resolution (m)					
	$I = 6, J = 4$	Upper	300	1/18	1/88		
		Axial	800	1/1	1/6		
		Deep	1400	1/5	1/25		
3	Even and odd loops	Fine resolution (m)					
	$I = 16, J = 10$	Top	80	0.5/3	0.5/17		
	$K = 8$	Upper	125	0.8/10	0.8/25		
		Axial	600	1/1	1/6		
		Deep	500	0.8/3	0.8/15		
		Bottom	500	0.5/1	0.5/5		
1b	Thermal wind						
	Even loops only	Fine resolution (m)					
	$I = 6, J = 10$	Upper	100	0.6/2	0.7/25	0.99/2.5	0.95/25
		Axial	600	1/1.6	1/6	1/1.6	1/6
		Deep	500	0.9/0.6	0.8/9	0.5/0.5	0.6/10

The listed temperature and velocity error bars are proportional to the travel-time error bar, assumed to be 1 ms throughout. This is optimistic, but of more concern is the use of the reference sound channel as a basis for all model calculations. Real profiles are more structured and can lead to difficulties in the interpretation of the arrival pattern. So we regard the present calculations as a reference against which future performance can be compared.

For orientation, modern oceanographic instruments have temperature and velocity uncertainties of the order of 5 m°C and 5 mm s^{-1}. Compared to these, the tomographic summary table generally gives smaller temperature and larger velocity errors. But this is not the principal consideration; it is rather that the horizontal and vertical averaging of tomography completely suppresses internal wave noise, whereas for ocean spot measurements, typical r.m.s. values are shown below.

	Temperature (m° C)	Velocity (mm s^{-1})
Upper ocean	150	50
Axial depth	30	30
Deep ocean	1	8

It is apparent that the computed tomographic error bars are below internal wave noise.

The case of six even-looped rays in a 10-layer ocean serves as our standard (1a). Only the axial layers are resolved; this means that we have taken them too thick (600 m). If there is no information other than the acoustic measurements (the agnostic case), then this standard case fails at other depths from lack of resolution. This does not mean that a layer cannot be resolved from its neighbor, but rather that it cannot be resolved from its conjugate (a layer of equal sound speed on the opposite side of the sound minimum axis) as shown by the VV^T matrix. We refer to this as the up–down ambiguity; without further information there is no way of knowing whether the perturbation in ray travel time comes from disturbances near the upper or the lower turning points. In this underdetermined case the inversion process then uses its degrees of freedom to apportion the disturbances almost equally among conjugate layers.

There are two ways to go: one is to reduce (or remove) the indeterminacy; the other is to impose our previous experience by selecting one out of an infinity of possible solutions.

The first way is termed agnostic. The simplest procedure is to reduce the number of layers, here from 10 to 4 (case 2). The case is now overdetermined and accordingly there is no ambiguity, at the expense of increased (but still acceptable) error bars. Another procedure is to stay with the 10 layers but to increase the number of rays by including odd loops.

Using the additional 10 rays with odd loops (plus the standard six even-looped rays) to increase the rank from 6 to 10, the problem is determined and resolution is everywhere one, but we then find unacceptably high error bars in the top layer: 0.1°C and 500 mm s^{-1}. The summary table is for the case where the odd loops are used to increase the rank from 6 to 8, so the inversion is still underdetermined. We now have acceptable error bars and good resolution in all but the top and bottom layer.

We can also take advantage of a known relation (the thermal-wind equation) to reduce the indeterminacy. As a result, case 1b is 80% determined (as is case 3), compared with 60% for the standard case 1a (by percent determinacy we mean the ratio of the rank to the number of unknowns). There are notable improvements in the deep ocean, but the upper ocean is still not adequately resolved.

By a suitable combination of the thermal-wind constraint plus a few odd loops and possibly a slight reduction in the number of layers, one can probably achieve adequate resolution with

acceptable error bars for the agnostic inversion. We are planning an experiment on long-term (climatic) changes where nothing is known about the relative warming (or cooling) at different depths, and the agnostic procedure would then be proper. However, in the case of mesoscale fluctuations (for example), a great deal is known: nearly all the fluctuations can be associated with the barotropic and the lowest baroclinic modes, and this suggests some version of mode weighting (the orthodox procedure) and will lead to satisfactory resolution of all 10 layers [this was done by THE OCEAN TOMOGRAPHY GROUP (1982), although with a slightly different procedure]. As an intermediate between the agnostic and orthodox inversions, N weighting leads to excellent results for the upper and axial ocean but to poor results for the deep ocean. Imposing the thermal-wind constraint helps with the deep ocean.

The appropriate depth weighting is a rational and consistent way of imposing on the inversion process the fact that something was known about the ocean prior to acoustic tomography. Properly done, such weighting is an asset, not a liability.

The vertical resolution problem is an open-ended one. We have described elsewhere (MUNK and WUNSCH, 1982) the application of tomography to large-scale determination of vorticity, potential vorticity as a function of depth, the determination of the vertical component of velocity, the direct measurement of velocity temperature correlations, etc. For each of these problems the issue of vertical resolution has to be faced. In all cases the procedure is a generalization of the one described here and is a function both of the measurement error and of the physics that can be assumed to be known. An asset of our procedure is that we can systematically improve our estimates of all quantities as our knowledge of the ocean improves.

Acknowledgements—This paper was prepared while we both enjoyed the hospitality of the Department of Applied Mathematics and Theoretical Physics, University of Cambridge, supported by the Fulbright program. In addition, CW acknowledges the support of the John Simon Guggenheim Foundation and the Natural Environment Research Council. The incentive for the work came from a series of experiments supported by the Office of Naval Research and the National Science Foundation. BARBARA GRANT carried out the numerical computations at MIT.

REFERENCES

CORNUELLE B. (1982) Ph.D. Thesis, MIT/WHOI, in preparation.

FOFONOFF N. P. (1962) Dynamics of ocean currents. In: *The sea: ideas and observations on progress in the study of the seas, 1: Physical oceanography*, M. N. HILL, editor, Wiley, Interscience, New York, pp. 323–395.

THE MODE GROUP (1978) The Mid-Ocean Dynamics Experiment. *Deep-Sea Research*, **25**, 859–910.

MUNK W. (1974) Sound channel in an exponentially stratified ocean, with application to SOFAR. *Journal of the Acoustical Society of America*, **55**, 220–226.

MUNK W. H. and C. WUNSCH (1979) Ocean acoustic tomography: a scheme for large-scale monitoring. *Deep-Sea Research*, **26**, 123–161.

MUNK W. and C. WUNSCH (1982) Observing the ocean in the 1990's. *Philosophical Transactions of the Royal Society of London*, **A**, in press.

THE OCEAN TOMOGRAPHY GROUP (1982) A demonstration of ocean acoustic tomography. *Nature*, **299**, 121–125

SCHOTT F. and H. STOMMEL (1978) Beta spirals and absolute velocities in different oceans. *Deep-Sea Research*, **25**, 961–1010.

WORCESTER P. F. (1977) Reciprocal acoustic transmission in a mid-ocean environment. *Journal of the Acoustical Society of America*, **62**, 895–905.

WUNSCH C. (1978) The general circulation of the North Atlantic west of 50°W determined from inverse methods. *Reviews of Geophysics and Space Physics*, **16**, 583–620.

WUNSCH C. (1980) Properties for inverse analysis of sound propagation in simple oceanic waveguides. *Journal of Marine Research*, **38**, 413–433.